ELECTRONIC SUPPORTING INFORMATION

The elusive silica/water interface: isolated silanols under water as revealed by vibrational sum frequency spectroscopy.

Laetitia Dalstein, Elizaveta Potapova, and Eric Tyrode*

Department of Chemistry, School of Chemical Science and Engineering,
KTH Royal Institute of Technology, SE-100 44 Stockholm, Sweden

* Corresponding author: tyrode@kth.se. Telephone: +46 8 7909915

Content:

1. Additional experimental details

Handling of silica substrates: prior to any pre-treatment (i.e. heat or plasma) all hemispheres were cleaned following this procedure: sonication in ethanol, thorough rinse in ultrapure water, immersion in chromosulphuric acid, and finally, once again, thorough rinse and sonication in water (see main article for additional details). During this procedure, hemispheres were placed inside Teflon beakers to avoid scratching the surfaces.

a) **Heat treatment:** hemispheres were placed inside a porcelain crucible and introduced into the oven at room temperature (Thermolyne-47900-Furnace). The temperature was thereafter ramped up to 1000ºC and left for 4 hours at the set value. The current supply was subsequently turned off, leaving the hemisphere inside the oven to cool-down overnight. The hemisphere was then kept dry (i.e. atmospheric air) in a Teflon beaker until measurements were performed. Note, that as mentioned in the main article, the hemisphere was immersed in chromosulphuric acid for 5 minutes, and thoroughly rinsed and sonicated in water just before assembly in the gas-tight measuring cell. This was required to remove organic contamination adsorbed while exposed to air following the heat treatment. Organic contamination could be easily detected in our high resolution SF spectrometer.

   Spectral features: No noticeable changes were observed in the SF spectra when immersing the heat treated hemisphere in water for more than 6 hours. Actually, even after boiling the hemisphere in water for several hours, only limited changes, if any, could be observed in the spectral features. This suggest that the formation of additional silanol groups (i.e. non-isolated) is slow in these flat extended surfaces. Having said this, plasma cleaning the sample for just a few minutes was sufficient to fully rehydroxylize the surface, as judged by the resulting SF spectra.

b) **Plasma cleaning:** hemispheres were introduced wet into the plasma cleaner (Harrick, PDC-32G, medium level, using air as carrier gas) and left inside for a total of ten minutes. Once removed from the plasma chamber, they were immediately immersed into water. Note that as for the heat treated samples, the plasma cleaned hemispheres were also immersed in chromosulphuric acid and copiously rinsed with water just before performing the measurements. As mentioned in the main article, we found the procedure to be reversible, in the sense that the spectral features could be recovered by plasma or heat treating the same silica sample.

2. Selective enhancement of spectral features in the SF spectra: Fresnel factor correction

The general theory of VSFS has been described in detail elsewhere,[2-5] and only a brief summary is presented here to explain the angular-dependent selective enhancement of spectral features in the SF spectra.[6]

The intensity of the SF beam in a co-propagating geometry is described by Equation [1], where I_i refers to the intensities of the incident fields, $\boldsymbol{\chi}_{eff}^{(2)}$ to the effective susceptibility tensor, $n_1(\omega_i)$ to the refractive indices of the incident media, and β_i to the angle of incidence (or emission) of the respective beams relative to the surface normal.

$$I_{SF}(\omega_{SF}) = \frac{8\pi^3\omega^2\sec^2\beta_{SF}}{c^3 n_1(\omega_{SF})\, n_1(\omega_{VIS})\, n_1(\omega_{IR})} \left|\chi_{eff}^{(2)}\right|^2 I_1(\omega_{VIS})\, I_2(\omega_{IR}) \tag*{[1]}$$

The tensors $\boldsymbol{\chi}_{eff}^{(2)}$ and $\boldsymbol{\chi}^{(2)}$ are related by the unit polarization vectors, $\hat{\mathbf{e}}$, and the Fresnel tensor $\mathbf{L'}(\omega)$:

$$\boldsymbol{\chi}_{ijk,eff}^{(2)} = \left[\mathbf{e}_i \mathbf{L}'_{ii}(\omega_{SF})\right] \cdot \boldsymbol{\chi}_{ijk}^{(2)} : \left[\mathbf{L}'_{jj}(\omega_{VIS})\,\mathbf{e}_j\right]\left[\mathbf{L}'_{kk}(\omega_{IR})\,\mathbf{e}_k\right] \tag*{[2]}$$

Expanding equation [2] for the tensor elements that are nonzero in isotropic interfaces gives:

$$\chi_{eff,SSP}^{(2)} = L'_{YY}(w_{SF})\, L'_{YY}(w_{VIS})\, L'_{ZZ}(w_{IR}) \sin\beta_{IR}\, \chi_{yyz}^{(2)} \tag*{[3]}$$

$$\chi_{eff,SPS}^{(2)} = L'_{YY}(w_{SF})\, L'_{ZZ}(w_{VIS})\, L'_{YY}(w_{IR}) \sin\beta_{VIS}\, \chi_{yzy}^{(2)} \tag*{[4]}$$

$$\begin{aligned}
\chi_{eff,PPP}^{(2)} = & -L'_{XX}(w_{SF})\, L'_{XX}(w_{VIS})\, L'_{ZZ}(w_{IR}) \cos\beta_{SF} \cos\beta_{VIS} \sin\beta_{IR}\, \chi_{xxz}^{(2)} \\
& -L'_{XX}(w_{SF})\, L'_{ZZ}(w_{VIS})\, L'_{XX}(w_{IR}) \cos\beta_{SF} \sin\beta_{VIS} \cos\beta_{IR}\, \chi_{xzx}^{(2)} \\
& +L'_{ZZ}(w_{SF})\, L'_{XX}(w_{VIS})\, L'_{XX}(w_{IR}) \sin\beta_{SF} \cos\beta_{VIS} \cos\beta_{IR}\, \chi_{zxx}^{(2)} \\
& +L'_{ZZ}(w_{SF})\, L'_{ZZ}(w_{VIS})\, L'_{ZZ}(w_{IR}) \sin\beta_{SF} \sin\beta_{VIS} \sin\beta_{IR}\, \chi_{zzz}^{(2)}
\end{aligned} \tag*{[5]}$$

The macroscopic Fresnel factors L_{nn} are defined according to the three layer model:[3,6]

$$L_{XX}(\Omega) = \frac{2n_1(\Omega)\cos\gamma}{n_1(\Omega)\cos\gamma + n_2(\Omega)\cos\beta} \tag*{[6]}$$

$$L_{YY}(\Omega) = \frac{2n_1(\Omega)\cos\beta}{n_1(\Omega)\cos\beta + n_2(\Omega)\cos\gamma} \tag*{[7]}$$

$$L_{ZZ}(\Omega) = \frac{2n_2(\Omega)\cos\beta}{n_1(\Omega)\cos\gamma + n_2(\Omega)\cos\beta} \cdot \left(\frac{n_1(\Omega)}{n'}\right)^2 \tag*{[8]}$$

In these equations, Ω is the wavelength, γ is the refracted angle, and n' is the refractive index of the infinitely thin polarization sheet in between the two bulk media.

We have previously illustrated by simulations and experiments[6] that the choice of the incident angles (β_i) of the IR and VIS beams has a large effect on the overall intensity of the SF signal and the relative enhancement of the spectral features across the probed frequency range.

In the present study, the incident angles of the IR and VIS beams were 55° and 70°, respectively, and were chosen to preferentially enhance the OH stretching region between 3600-3800 cm^{-1}, where the silanol peaks are located. This enhancement is accounted for by the Fresnel prefactor in Equation [9].

$$Fresnelprefactor = \frac{\omega_{SF}^2 \sec^2 \beta_{SF}}{c^3 n_1(\omega_{SF}) n_1(\omega_{VIS}) n_1(\omega_{IR})} \left|\chi_{eff}^{(2)}\right|^2 \qquad [9]$$

The relative enhancement for different polarization is shown graphically in Figure S1, for the H_2O/silica and D_2O/silica interfaces, respectively. While the SSP and SPS polarization combinations only contain contributions from one susceptibility tensor element each (assuming C_∞-symmetry of the interface), the PPP is an admixture of four tensor elements. In the curves for the spectral normalization shown in Figure S1, only the zzz-element is included since it is expected to the substantially larger than the other elements.

The refractive indices of silica in the IR and SF ranges were calculated using the Selmeier equation (the imaginary term was assumed to be zero).[7] $n_{silica,\ 800\ nm}$ was set to 1.453.

The real (n) and imaginary (k) parts of the refractive indices of water and deuterium oxide were adopted from Segelstein,[8] and the complex refractive index (n_c) was calculated as $n_c = n + ik$. n' was set to 1.4 for the IR, VIS, and SF ranges.

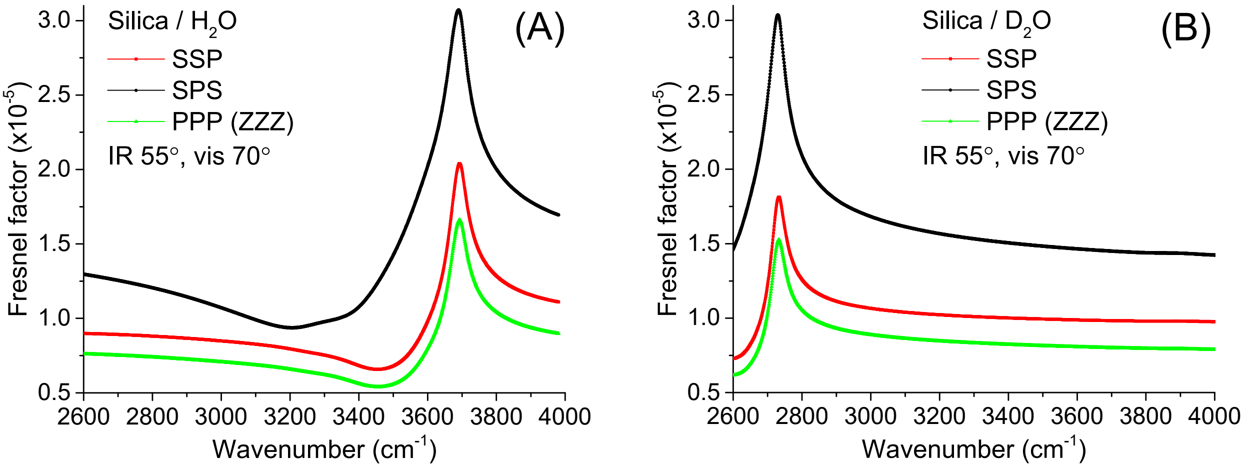

Figure S1. Fresnel prefactor corrections for the (A) fused silica/H_2O and (B) fused silica/D_2O interfaces. Note the clear enhancement at the frequency range of interest. These curves were used to normalize the recorded VSF spectra and remove the frequency dependent enhancement as shown in the following section.

3. Fresnel factor corrected VSF spectra.

The figures in this section corresponds to Figures 1, 2, and 4, in the main paper, which here have been corrected to account for the refractive index and experimental geometry dependent factors as described in the previous section. The number(s) within parenthesis after each figure number denotes the corresponding figure number in the main paper. Note that the $\nu_{i\mathrm{SiOH}}$ at ~3680 cm^{-1} remains visible, at least as a shoulder, in all the Fresnel factor corrected spectra.

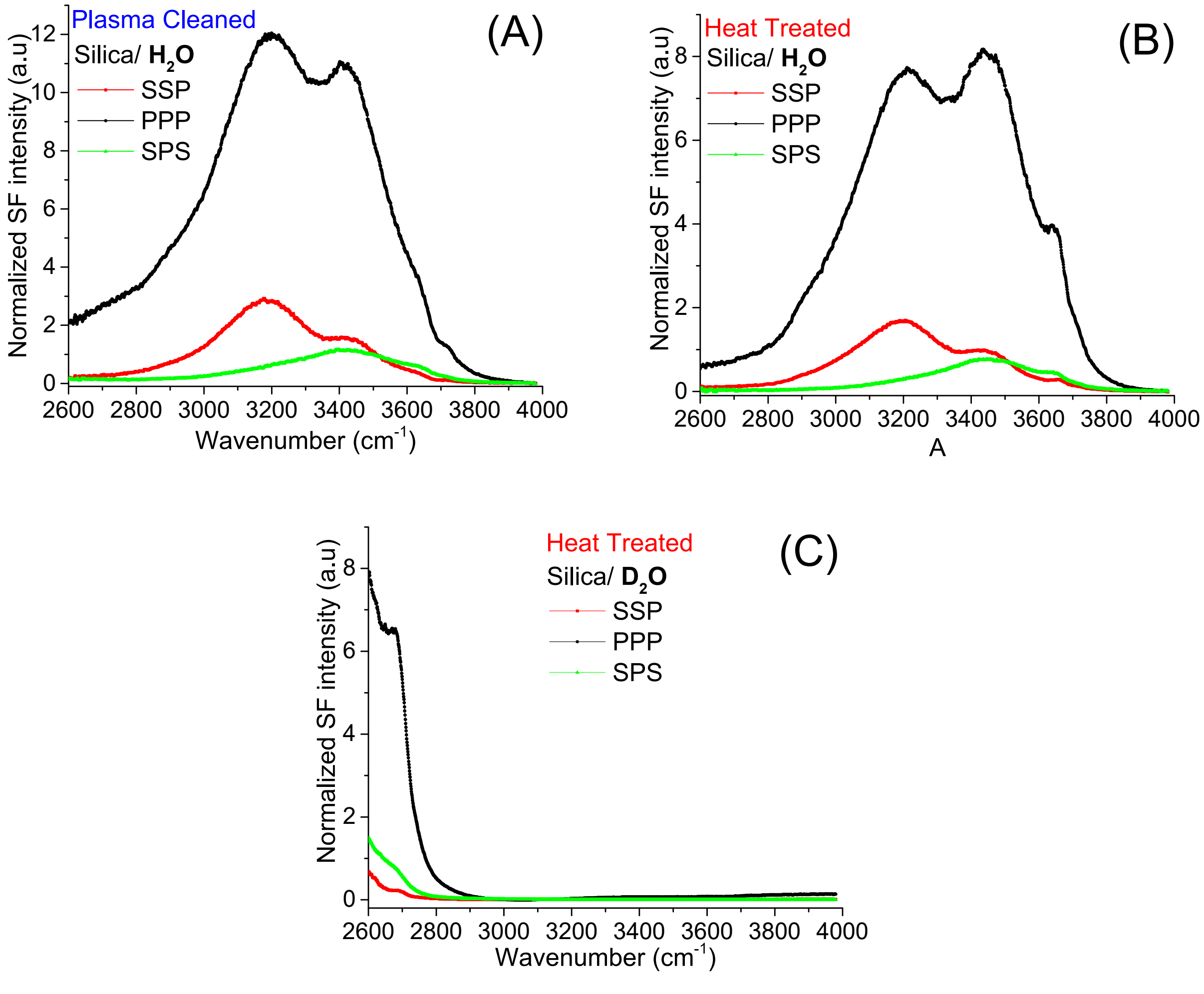

Figure S2 (1a,1b,1c). Fresnel prefactor corrected VSF spectra recorded in the SSP, PPP, and SPS polarization combinations of the (a) plasma, and (b) heat treated fused silica in pure H_2O. (c)VSF spectra of heat treated silica in D_2O.

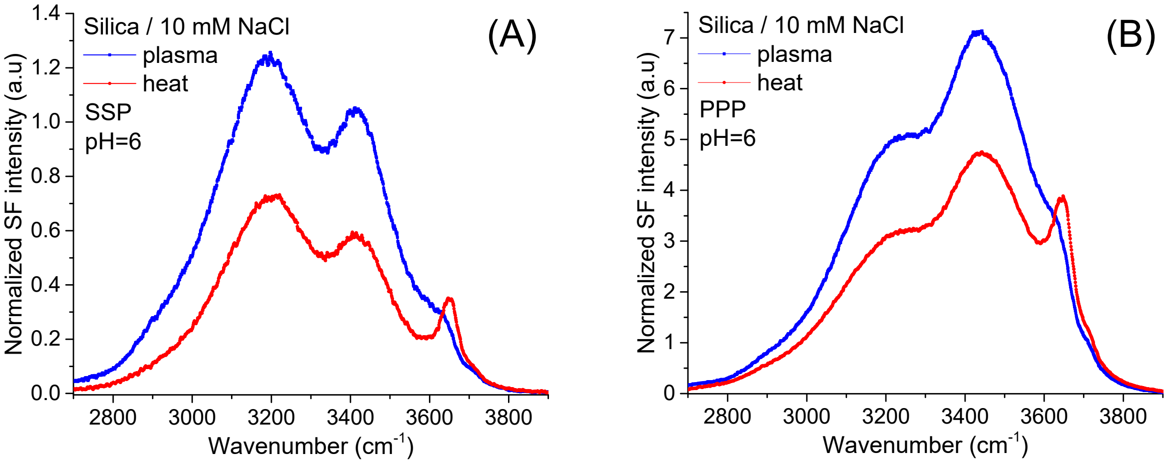

Figure S3 (2a,2b). Fresnel prefactor corrected VSF spectra recorded in the (a) SSP, and (b) PPP polarization combinations of plasma and heat treated fused silica in contact with 10 mM NaCl solution.

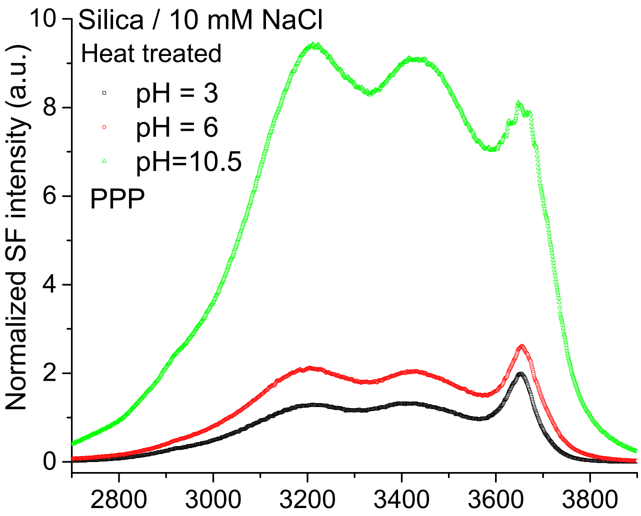

Figure S4. VSF spectra recorded in the PPP polarization combination of a heat treated fused silica in contact with 10mM NaCl solution at three different pHs. Note that these spectra have not been Fresnel factor corrected. The sharp features resolved on top of the $\nu_{i\mathrm{SiOH}}$ band at pH 10.5 are due to IR absorption from water vapour before reaching the sample position.

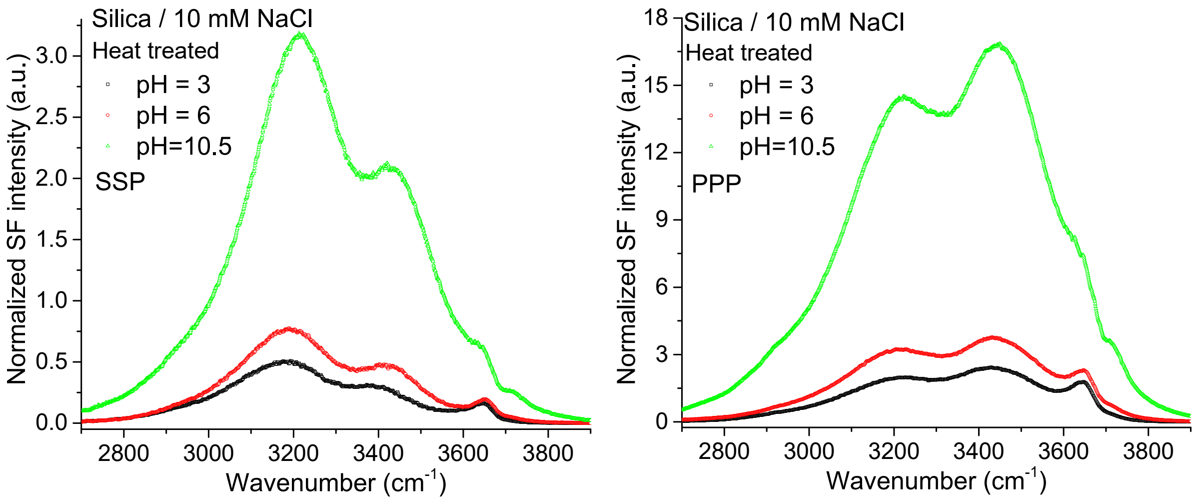

Figure S5 (4,S4). Fresnel prefactor corrected VSF spectra recorded in the (a) SSP, and (b) PPP polarization combinations of a heat treated fused silica substrate in contact with 10mM NaCl solution at three different pHs. The $\nu_{i\mathrm{SiOH}}$ band remains apparent, even at pH 10.5.

4. Fitting methods and results

As mentioned in the main article, the spectra presented in Figures 4 and 5 were fitted by convoluted Lorentzian and Gaussian line shapes, that accounts for homogeneous (Lorentzian line shapes) and inhomogeneous broadening (Gaussian line shape), as well as the complex interference between neighbouring bands.

As bands in the OH stretching region are typically dominated by inhomogeneous broadening ($\sigma_v > \Gamma_v$), we set Γ_v to 15 cm^{-1}. The spectra presented in Figure 4 and Figure 5 of the main manuscript, were fitted using only three resonant bands. It is however, recognized that additional bands may most certainly contribute to the SF intensity in this region (i.e. at ~3500 cm^{-1} there is a band clearly resolved in the SPS spectrum that will have a non-negligible contribution at high pH in the SSP spectra). Increasing the number of bands improves the quality of the fit, but at the expense of obtaining less reliable fitting values. Having said this, regardless of how the spectra in Figure 4 are fitted, the main point is that the ~ 3680 cm^{-1} peak from surface silanols follows a different trend (i.e. remains approximately constant) and has an amplitude of opposite sign to those from water bands at lower frequencies. In Figure 5, however, for the CTAB spectra when the surface is positively charged, the three bands have the same sign, consistent with the isolated silanol assignment.

The fitted parameters for Figure 4 are summarized in the table below (heat treated silica, SSP):

pH	A_1	ω_1(cm^{-1})	σ_1 (cm^{-1})	A_2	ω_2(cm^{-1})	σ_2 (cm^{-1})	A_3	ω_3(cm^{-1})	σ_3 (cm^{-1})	A_{NR}
3.0	57.9	3203	116	6.9	3404	44.6	-10.8	3686	23.9	0.01
6.0	76.2	3214	118	9.2	3416	46.5	-13.4	3693	29.4	0.04
10.5	128.8	3231	120	15.7	3431	49.4	-25.6	3686	52.4	0.16

pH	A_1/σ_1	A_2/σ_2	A_3/σ_3
3.0	0.50	0.15	-0.45
6.0	0.65	0.20	-0.46
10.5	1.07	0.32	-0.49

The fitted parameters for Figure 5 are summarized in the table below (heat treated silica, PPP):

	A_1	ω_1(cm^{-1})	σ_1 (cm^{-1})	A_2	ω_2(cm^{-1})	σ_2 (cm^{-1})	A_3	ω_3(cm^{-1})	σ_3 (cm^{-1})	A_{NR}
CTAB 2 mM	-202	3261	110	-274	3526	100	-11	3682	14	0.12
NaCl 10 mM	159	3245	120	54	3430	72	-39	3683	26	0.13

5. References

1. Isaienko, O.; Borguet, E. Hydrophobicity of Hydroxylated Amorphous Fused Silica Surfaces. *Langmuir* **2013,** *29* (25), 7885-7895.
2. Bain, C. D. Non-linear optical techniques. In *Surfactant Science Series*, Dekker: New York, 1999; Vol. 83, pp 335-373.
3. Zhuang, X.; Miranda, P. B.; Kim, D.; Shen, Y. R. Mapping molecular orientation and conformation at interfaces by surface nonlinear optics. *Physical Review B: Condensed Matter* **1999,** *59* (19), 12632-12640.
4. Richmond, G. L. Molecular Bonding and Interactions at Aqueous Surfaces as Probed by Vibrational Sum Frequency Spectroscopy. *Chemical Reviews* **2002,** *102* (8), 2693-2724.
5. Lambert, A. G.; Davies, P. B.; Neivandt, D. J. Implementing the Theory of Sum Frequency Generation Vibrational Spectroscopy: A Tutorial Review. *Applied Spectroscopy Reviews* **2005,** *40* (2), 103-145.
6. Liljeblad, J. F. D.; Tyrode, E. Vibrational Sum Frequency Spectroscopy Studies at Solid/Liquid Interfaces: Influence of the Experimental Geometry in the Spectral Shape and Enhancement. *The Journal of Physical Chemistry C* **2012,** *116* (43), 22893-22903.
7. Malitson, I. H. Interspecimen Comparison of the Refractive Index of Fused Silica. *J. Opt. Soc. Am.* **1965,** *55* (10), 1205-1208.
8. Segelstein, D. J. The complex refractive index of water. Master Thesis. University of Missouri, USA, Kansas City, 1981.